Immobilization of a molecular Re complex on MOF-derived hierarchical porous carbon for CO_2 electroreduction in water/ionic liquid electrolyte

*Domenico Grammatico,[1 3] Huan Ngoc Tran,[2] Yun Li,[2] Silvia Pugliese,[1 2] Laurent Billon, [3] Bao-Lian Su [1 *] and Marc Fontecave [2 *]*

[1] Laboratory of Inorganic Materials Chemistry (CMI), University of Namur, 61 rue de Bruxelles, B- 5000 Namur, Belgium.

[2] Laboratoire de Chimie des Processus Biologiques, UMR CNRS 8229, Collège de France-CNRS-Sorbonne Université, PSL Research University, 11 Place Marcelin Berthelot, 75005 Paris, France.

[3] Bio-inspired Materials Group: Functionality & Self-assembly, Universite de Pau et des Pays de l'Adour, E2S UPPA, CNRS, IPREM UMR 5254, 64000, PAU, France

* to whom correspondence should be addressed : marc.fontecave@college-de-france.fr; bao-lian.su@unamur.be

KEYWORDS: CO_2 electroreduction; catalysis; rhenium complex; heterogenization; hierarchical porous carbon

Abstract

The development of molecular catalysts for CO_2 electroreduction within electrolyzers requests their immobilization on the electrodes. While a variety of methods have been explored for the heterogenization of homogeneous complexes, we here report a novel approach using a hierarchical porous carbon HPC material, derived from a Metal Organic Framework, as a support for the well-known molecular catalyst [Re(bpy)$(CO)_3$Cl] (bpy = 2,2'-bipyridine). This cathodic hybrid material, named HPC@Re, has been tested for CO_2 electroreduction using a mixture of an ionic liquid (1-Ethyl-3-methylimidazolium tetrafluoroborate EMIM) and water as the electrolyte. The present study reveals that HPC@Re is a remarkable catalyst, enjoying excellent activity (high current densities and high turnover numbers) and good stability. Interestingly, it catalyzes the conversion of CO_2 into a mixture of carbon monoxide and formic acid, with a selectivity that depends on the applied potential. These results emphasize the advantages of integrating molecular catalysts onto such porous carbon materials for developing novel, stable and efficient, catalysts for CO_2 reduction.

Introduction

Carbon dioxide electroreduction into energy-dense carbon-based liquid or gaseous products is an attractive way to store renewable energies into chemical energy. However, because of the high stability of CO_2 and the requirement of multiple electron and proton-transfers for its transformation, catalysts are required to overcome the slow kinetics, minimize overpotentials and control product selectivity. While heterogeneous catalysts are generally favored due to their stability as well as facile product and catalyst recovery, homogeneous molecular metal complexes (coordination and organometallic complexes) have also been developed since the 1980's. In particular, they offer the unique opportunity to tune the coordination environment of the metal center and its reactivity *via* synthetic modifications of the ligands. The molecular strategy has been recently described in review articles.[1,2]

To reconcile these two approaches, homogeneous catalysts have sometimes been immobilized on heterogeneous conductive supports. However, this strategy has been applied to few molecular catalysts with limited success so far.[3–5] To illustrate the various techniques developed for providing access to modified electrodes, the case of the prototypical catalyst [Re(bpy)$(CO)_3$Cl] (bpy = 2,2'-bipyridine), highly selective for CO_2 to CO conversion, is interesting, since its immobilization has been studied using a variety of approaches. The first attempts to immobilize such complexes were achieved by Meyer and coworkers [6] and Abruña and coworkers [7] in 1985 and 1986, respectively, two years after the initial publication by Lehn reporting the catalytic activity of this complex for CO_2 reduction.[8] In both cases, the catalyst was immobilized *via* electropolymerization of [Re(vbpy)$(CO)_3$Cl] (vbpy = 4-vinyl-4'-methyl-2,2'-bipyridine) on an electrode to afford catalytic poly-[Re(vpbpy)(CO)Cl] films, allowing electroreduction of CO_2 to CO with very high faradaic yields in CH_3CN. However, these films were shown to exhibit limited stability. A similar polymerization approach was recently developed by Kubiak and co-workers using 5-ethynyl-bipyridine derivatives, instead of vinyl-bipyridine, however, in that case very fast deactivation of the catalytic films was observed.[9] A different strategy for electropolymerization of a variant of Re(bpy)$(CO)_3$Cl was reported by Deronzier and co-workers.[10] Upon electrochemical oxidation of a solution of Re(pyrbpy)$(CO)_3$Cl (pyrbpy = 4-(4-Pyrrol-l-ylbuty1)4'-methyl-2,2'-bipyridine) using a Pt electrode, a polypyrrole-based film was deposited and found to catalyze the electroreduction in CH_3CN of CO_2 leading to CO as the only reduction product. However, the polymer was highly unstable and substantial loss of current was observed during electrolysis. In 1993, Kaneko and co-workers reported the immobilization, *via* simple adsorption, of Re(bpy)$(CO)_3$Br within a

Nafion© membrane, which is conductive and stable in various solvents and easily interfaces with electrode surfaces.[11] The polymer-confined catalyst was active for CO_2 electroreduction in neutral aqueous electrolyte, leading to mixtures of CO, H_2 and formic acid, with a selectivity depending on the applied potential.

Besides this immobilization involving polymers and membranes, covalent grafting to the electrode has also been explored. As *o*-quinone moieties found on the edge planes of graphite can condense with substituted *o*-phenylenediamines, Re(5,6-diamino-phenanthroline)$(CO)_3Cl$ was used to modify graphite electrodes.[12] The increased conjugation between the catalyst and the electrode was proposed to overcome poor conductivity issues in other polymeric films deposited onto electrodes. This system was very selective for CO formation (faradaic yield of 96%) in CH_3CN with high TONs. A conjugated polymer material incorporating Re(bpy)$(CO)_3Cl$ motifs and covalently attached to a glassy carbon electrode was obtained by electropolymerization of a Re complex containing 2,2'-bipyridine-5,5'-bis-(diazonium) ligands.[13] These molecular films proved highly stable, allowing thousands of turnovers for selective production of CO in CH_3CN.

Finally, non-covalent immobilization was achieved, exploiting π-π interactions between pyrolytic graphite and Re(pyrene-bpy)$(CO)_3Cl$, containing a pyrene-substituted bpy.[14] This system was catalytically active for CO production but was rapidly deactivated, likely because of reduction of the pyrenyl moiety. The best result with such a non-covalent immobilization strategy was obtained by Kubiak and co-workers who developed a hybrid electrode resulting from the incorporation of Re(tBu-bpy)$(CO)_3Cl$, with tBu-bpy = 4,4'-di-*tert*-butyl-2,2'-bipyridine, into multi-walled carbon nanotubes (MWCNTs). This material proved stable and active in an aqueous electrolyte for highly selective CO production, at relatively low overpotential and with a current density of 4 $mA.cm^{-2}$.[15]

One of the drawbacks of all these immobilization strategies, with the exception of the MWCNT/ Re(tBu-bpy)$(CO)_3Cl$ system, resides in the need to introduce functionalities to the bipyridine ligand. This not only generates synthetic issues but also results in significant modifications of the electronic properties of the catalyst as well as of its reactivity. We thus thought of developing methods that allow the immobilization of the [Re(bpy)$(CO)_3Cl$] itself without synthetic modifications. Here we report the preparation and characterization of an original conductive carbon porous material and its utilization as a support for the [Re(bpy)$(CO)_3Cl$] catalyst, which can be easily fixed within the pores of the solid material. The novel hybrid material proved stable and active as a catalyst for CO_2 electroreduction, with high current

densities and high turnover numbers. Interestingly, this catalyst converts CO_2 into a mixture of CO and HCOOH, whose ratio depends on the applied potential.

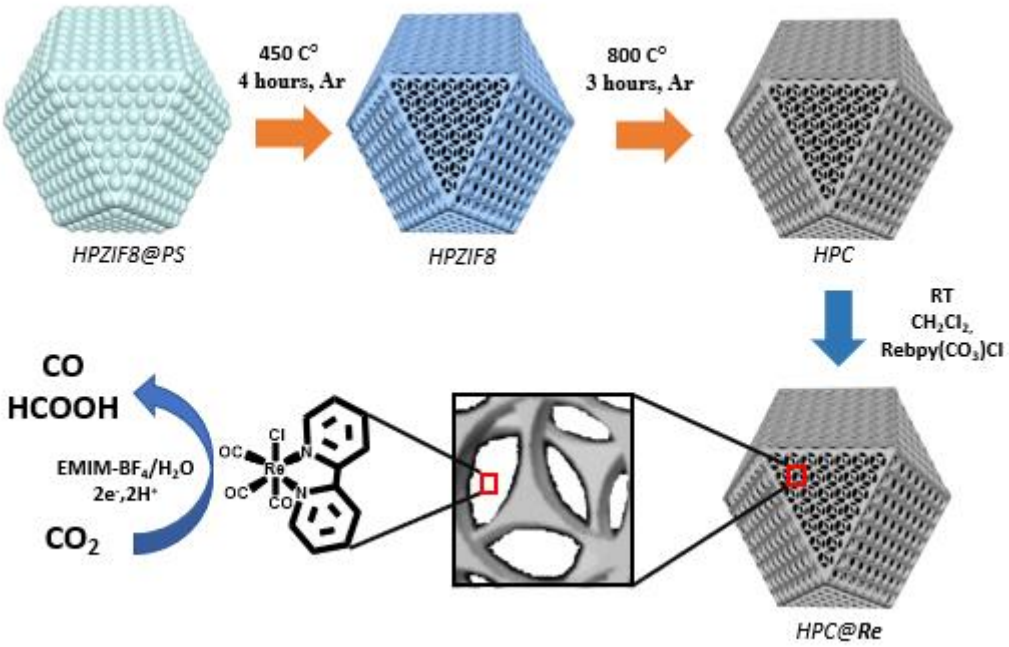

Scheme 1: Synthesis of HPC and HPC@Re.

RESULTS AND DISCUSSION

Synthesis and characterization of the hierarchical porous ZIF8-derived carbon-HPC

The synthesis of hierarchical porous carbon (named HPC in the following) derived from the Metal Organic Framework ZIF8 was synthesized following a previous report,[16] however with significant modifications (Scheme 1). First, the ZIF8 precursor was infiltrated into the polystyrene spheres (PS) template and crystallized using a solution of $CH_3OH/NH_3{\cdot}H_2O$. Second, a treatment at 450 °C under argon atmosphere, instead of washing with organic solvents used in the previous report,[16] was carried out in order to remove the PS template and thus obtain the hierarchical porous ZIF8 (HPZIF8). HPZIF8 shows slightly lower BET surface area (Figure S1 and Table S1) as compared to the previous report,[16] likely due to remaining PS beads in the sample. Scanning electronic microscope (SEM) and powder x-ray diffraction (XRD) characterizations of HPZIF8 show expected well-defined ZIF8 crystals (Figures S2-S3). HPZIF8 was finally pyrolyzed under inert atmosphere at 800 °C to obtain the final hierarchical porous carbon (HPC) material. HPC was characterized by various techniques. XRD pattern

confirmed that the material was not crystalline anymore (Figure S2). SEM images (Figure 1a) showed well-defined and well-distributed carbon particles with a three-dimensional tetrakaidecahedron morphology and with a uniform (monodisperse) diameter of 2 µm. This specific morphology is due to the use of PS latex as a template which controls the shape of the material.[16] The highly ordered porous carbon material showed a hexagonal-close-packed arrangement of PS nanospheres ??? (inset Figure 1a) with interconnected windows and porosity uniformly distributed.[17,18] N_2 physisorption analyses (Figure 1b and Figure S1) allowed to establish a BET surface area of 495 $m^2.g^{-1}$ and total pore volume of 1 $cm^3.g^{-1}$ with around 25% of the total pore volume assigned, by the Horwart-Kawazoe method, to the micropores. The increase of the surface area due to the pyrolysis step leading to HPC (495 $m^2.g^{-1}$) from HPZIF8 (145 $m^2.g^{-1}$) is likely due to a complete removal of PS. N_2 adsorption isotherms are of typical type I, indicating the microporous character of the material with a pore size located at 0.5 nm. The presence of mesopores and macropores has been revealed by two N_2 adsorption uptakes at p/p_o of 0.5 and 0.95-1.0, respectively, as shown in Figure 1b. The BJH analysis method gives a very sharp pic centered at 5 nm, corresponding to the hysteresis loop at p/p_o of 0.5 [19] while the sharp N_2 adsorption uptake at p/p_o of 0.95-1.0 is generated by the macropores of 380 nm observed by SEM (Figure 1a). The above analysis suggests HPC material contains a hierarchical macro-meso-microporous structure.

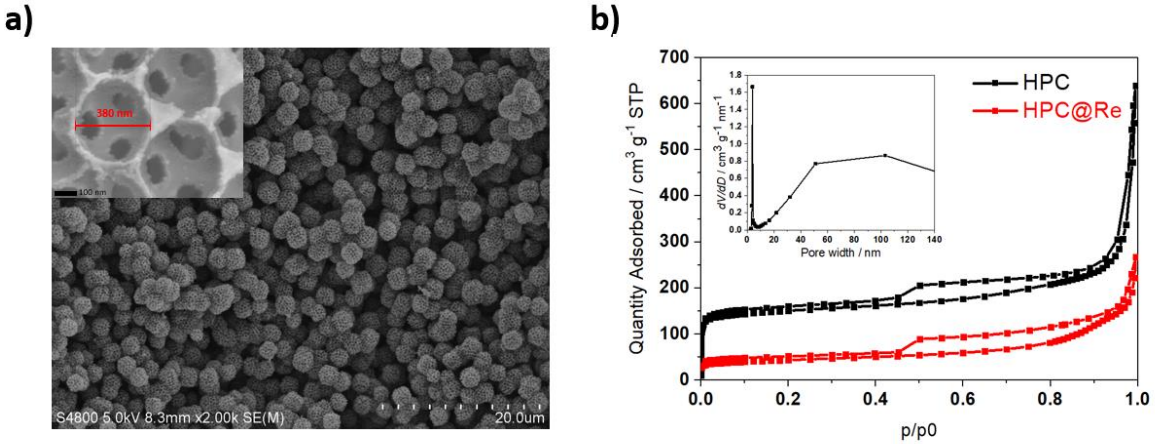

Figure 1: a) SEM image of HPC with enlargement (inset); **b)** N_2 adsorption-desorption isotherms of HPC and Re@HPC and pore size distribution (inset) made by BJH method of HPC.

Functionalization of HPC material with a molecular complex

HPC was then used as a support for heterogeneizing the molecular [Re(bpy)$(CO)_3$Cl] complex, named Re in the following. Re was immobilized without any further functionalization taking advantage of the interconnected porosity of the support which improves the hosting properties. The heterogenization of Re on HPC has been carried out as follows. First, Re was dissolved in CH_2Cl_2 and the solution added dropwise to a sonicated dispersion of HPC in the same solvent (Scheme 1). The solution was stirred for 1 hour and after centrifugation the supernatant removed. Finally, the as-obtained hybrid system was dried overnight at room temperature. The relative amounts of starting precursors were chosen in order to obtain an initial weight Re:HPC ratio of 1:9. Then, the obtained HPC@Re material was characterized not only to check for the presence of the molecular complex within the solid but also to define morphology and structure of the final material.

SEM images of Re@HPC showed that the morphology of the carbon particles was retained (Figure S4). The presence of Re within the solid has been verified by Energy Dispersive X-Ray mapping (EDX) (Figure S4) showing a uniform dispersion of the complex, as well as the presence of residual Zn from ZIF8, even after pyrolysis. N_2 physisorption analysis after Re loading showed a decrease of the BET surface area, indicating clearly the incorporation of the molecular complex within the pores of the support (Figure 1b). The integrity of Re within the solid material was proved by ^{1}H NMR spectroscopy after releasing the complex from Re@ HPC by washing with $CDCl_3$. The spectrum of the solution proved identical to that of the pure freshly prepared homogeneous complex (Figure S5). Finally, the amount of extractible complex from 30 mg of HPC@Re using an organic solvent (CH_2Cl_2) was determined by UV-Visible spectroscopy from the intensity of the absorption band at 387 nm, characteristic of the complex (Figure S6). It was determined by ICP-MS that the sample contained 4.8 µmol of complex leading to 0,16 µmol/mg of complex within Re@HPC.

Preparation and characterization of the working HPC@Re/GDL electrode

An Re@HPC /GDL electrode (1cm^2) was prepared by deposition of 5 mg HPC@Re on a commercial gas diffusion layer (GDL), as described in the experimental section. The total amount of Re in that electrode was determined by UV-Visible spectroscopy as described above for HPC@Re (Figure S6). The electrode was shown to contain 0.6 µmol.cm^{-2}. The CV of HPC@Re/GDL electrode in 0.1 M $TBAPF_6$ in CH_3CN at low scan rate of 10 mV.s^{-1} (Figure S7) served to calculate the density of electroactive species from the charge integration of the peak at about -1.6 V *vs* Fc/Fc$^+$, corresponding to the reoxidation of the complex.[20] The data

led to a high surface density of 20 nmol.cm^{-2}, corresponding to approximately 3% of the total amount of complex present in the solid material. These numbers compare well with those determined for the best hybrid [Re(tBu-bpy)(CO)$_3$Cl]/MWCNT material (13 nmol.cm^{-2}, 1-8% of the total catalyst loaded) reported by Kubiak *et al.*[15]

Electrocatalytic CO_2RR in water/1-Ethyl-3-methylimidazolium tetrafluoroborate (EMIM) electrolyte

Since the electroreduction of CO_2 using the HPC@Re/GDL in water yielded mainly hydrogen (data not shown), the reaction was studied in a CO_2-saturated solution of an ionic liquid in the presence of a small amount of water as a source of protons. Indeed, ionic liquids have been shown to facilitate CO_2 electroreduction catalyzed by solid catalysts due to their ability to increase CO_2 solubility and activate CO_2.[21] A previous report showed that using an ionic liquid as both the solvent and electrolyte resulted in decreased overpotential and increased second-order rate constant for CO_2 electroreduction to CO catalyzed by [Re(bpy)(CO)$_3$Cl].[22] However, with such homogeneous systems, the viscosity of the medium results in strong limitations in mass transport (small diffusion coefficients) of the molecular catalyst and low current densities. This issue does not apply to an immobilized molecular complex. Thus, a mixture of an ionic liquid (1-Ethyl-3-methylimidazolium tetrafluoroborate) and water (named H_2O/EMIM in the following) has been chosen as the electrolyte for further CO_2 electroreduction studies using the HPC@Re/GDL electrode. The Linear Sweep Voltammograms (LSVs) of the HPC@Re/GDL electrode in 5% v/v H_2O/EMIM saturated with either Ar or CO_2 are presented in Figure 2a. A catalytic wave at an onset potential of -1.55 V *vs* Fc/Fc$^+$ and developing further up to an applied potential of -2.05 V was observed only in the presence of CO_2 and was thus assigned to CO_2 reduction (Figure 2a). At potentials more negative than -2.1 V, a second wave was observed however also present for the HPC@Re/GDL electrode under argon, thus likely corresponding to proton reduction to H_2. Unfortunately, the evaluation of overpotential values is not trivial here as the equilibrium potentials of the CO_2/HCOOH and CO_2/CO couples in H_2O/EMIM are unknown.

Controlled Potential Electrolysis (CPE) at different potentials between -1.75 V and -2.05 V *versus* Fc/Fc$^+$ coupled with quantification of CO_2 reduction products has been carried out for 15 minutes in order to characterize the CO_2 reduction reaction. As expected the total current density increased with increased driving force up to 11 mA.cm^{-2} at -2.05 V and was found to be stable during electrolysis at all potentials (Figure 2b). The high current densities translate

into remarkably high turnover numbers (TONs) and high Turnover Frequencies (TOFs). For example, at -2.05 V, 2026 TONs are reached after 15 min, which corresponds to a TOF value of 2.3 s^{-1}. As shown below, under these conditions, formate was the major product.

The only detected products in all experiments were H_2 and CO in the gaseous phase and formic acid in the liquid phase. Surprisingly, the selectivity of the reaction was found to be greatly dependent on the applied potential, with CO being the major product at the most anodic potentials and formic acid becoming the major product at potentials more cathodic than -1.9 V, while H_2 was a minor product at all potentials. This is clearly shown in Figure 2c which displays the Faradic yields (FY) of the various products at different potentials. At -1.75 V *vs* Fc/Fc^+, FY(CO) and FY(H_2) were 79% (TON_{CO} 258 and TOF_{CO} 0.3 s^{-1}) and 9% respectively, and no formate could be found in the liquid phase. Screening the reaction at more negative potentials, CO formation decreased dramatically while FY(HCOOH) and FY(H_2), the latter to a smaller extent, increased. At -2.05 V, FY(CO), FY(H_2) and FY(HCOOH) were 3%, 20% and 76% (TON_{HCOOH} 1950 and TOF_{HCOOH} 2.2 s^{-1}) respectively (Figure 2c). Thus, the selectivity between CO *vs* HCOOH formation during electroreduction of CO_2 catalyzed by HPC@Re can be finely tuned by varying the applied potential.

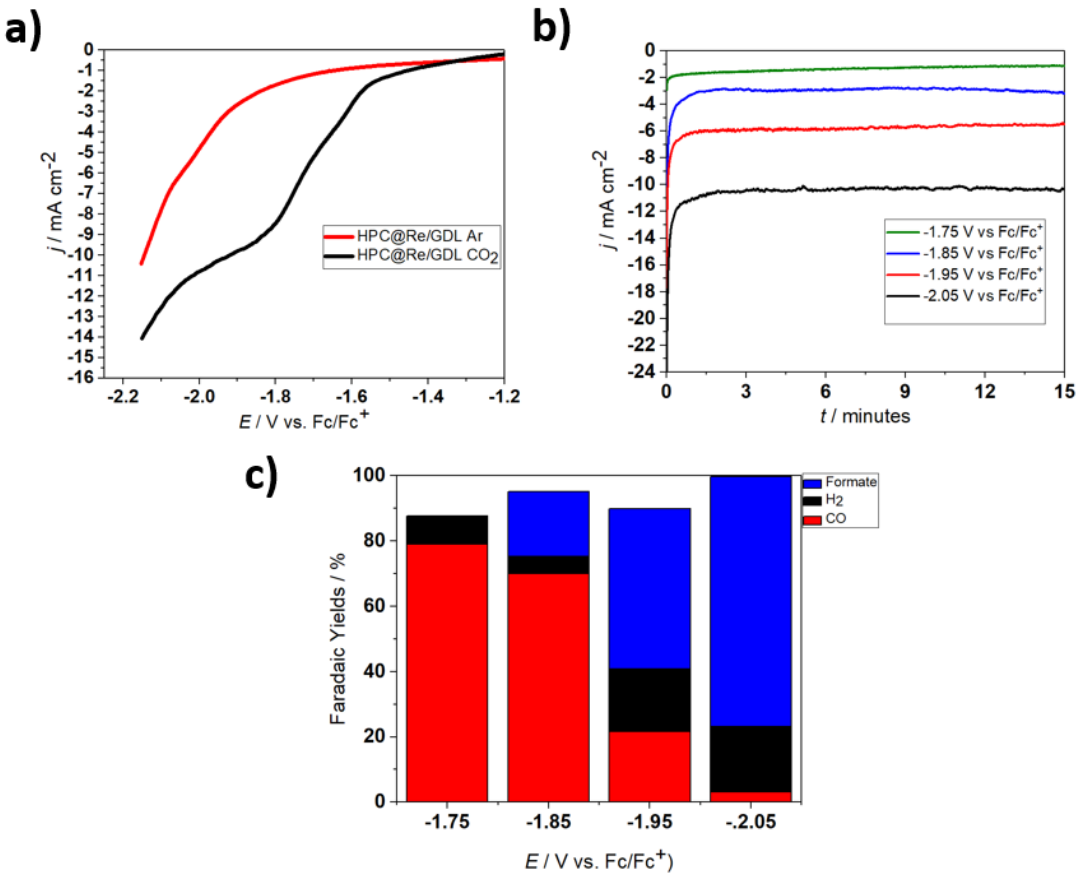

Figure 2: Controlled potential electrolysis of CO_2 using the HPC@Re/GDL electrode: **a)** LSV in 5% v/v H_2O/EMIM saturated with CO_2 (black) or with Ar (red), scan rate 20 $mV.s^{-1}$; **b)** total current density at various applied potentials as a function of time; **c)** Faradaic Yields for CO, H_2 and formate after 15 min electrolysis at different potentials in 5% v/v H_2O/EMIM saturated with CO_2.

The observation of formate formation is unexpected since the Re complex is known to be a very selective catalyst for CO_2 electroreduction to CO in organic solvents. Interestingly, when, as a control experiment, CPE was carried out using the soluble Re complex in the same CO_2-saturated 5% v/v H_2O/EMIM electrolyte, the reaction was shown to yield mainly H_2 with minor amounts of CO and almost no HCOOH, at all visited potentials (Figure S8). Furthermore, the current densities were much lower since at -1.85 V the current density reached a value of 0.3 $mA.cm^{-2}$ (Figure S8) for 12 μmol of Re catalyst (1 mM in 12 ml) as compared to 3 $mA.cm^{-2}$ for 0.6 μmol Re catalyst present in HPC@Re/GDL (Figure 2). This thus demonstrates the great impact of the solid support on the reaction outcome, both in terms of the activity and the selectivity. The effect on the activity is likely to be partly due to the hydrophobic nature of the environment provided by the pores in which the catalyst is bound, favouring CO_2 uptake and increasing CO_2 local concentration and to the absence of mass transport limitations which challenge the homogeneous catalyst.

In contrast, the effect of the solid support on the selectivity is difficult to explain. Formation of formate cannot be explained by the catalytic properties of the support itself since, as a control experiment, CPE of CO_2 using an HPC/GDL electrode, not loaded with the Re complex, under identical conditions, gave very different results (Figure S9). For example, at -1.85 V, with a current density of 1 $mA.cm^{-2}$, no formate could be detected, as compared to 3 $mA.cm^{-2}$ and a FY(HCOOH) of 20% for the HPC@Re/GDL electrode, and at -1.95 V, with a current density of 2 $mA.cm^{-2}$, a FY(HCOOH) of 15% was obtained, as compared to 6 $mA.cm^{-2}$ and a FY(HCOOH) of 50% for the HPC@Re/GDL electrode. There is, to our knowledge, one study reporting formate production during electroreduction of CO_2 catalyzed by the Re complex, with a HCOOH/CO selectivity depending on the applied potential as well.[11] Interestingly, in that case, the catalyst was incorporated into a Nafion membrane and electrolysis was carried out in a phosphate aqueous electrolyte, explaining why the major product at almost all potentials applied was H_2. The activity, in terms of current density, of that system was furthermore much lower than that reported here. While formate production using the HPC@Re catalyst is likely to proceed *via* a Re-H hydride species reacting with CO_2,[23,24] in contrast to CO production which derives from a Re-CO_2 intermediate, it is so far unclear why the HPC support favours

such a mechanism at very cathodic potentials and how the support tunes the HCOOH/CO selectivity. These mechanistic aspects deserve further investigation.

Finally, long-term CPE was carried out for 2 hours at -1.75 V (formation of CO and H_2) and -1.95 V (formation of CO, HCOOH, H_2) *vs* Fc/Fc^+ (Figure 3). The system proved very stable during electrolysis in terms of both current density and selectivity. After 2 hours at -1.75 V, 3155 TON_{CO} were achieved corresponding to a TOF_{CO} of 0.4 s^{-1}. Furthermore, post-electrolysis characterization of the electrode by SEM showed that the porosity of the system was retained even if slight agglomeration of the particles was observed (Figure S10). Finally, the amount of Re released in solution after 2 hours electrolysis was measured by ICP-MS and found to be within 5 to 10%, from one experiment to another, with respect to the initial amount of Re initially present on the electrode. Based on the results given above (Figure S8), this amount is far too small to account for the CO_2 reduction activity of the electrode.

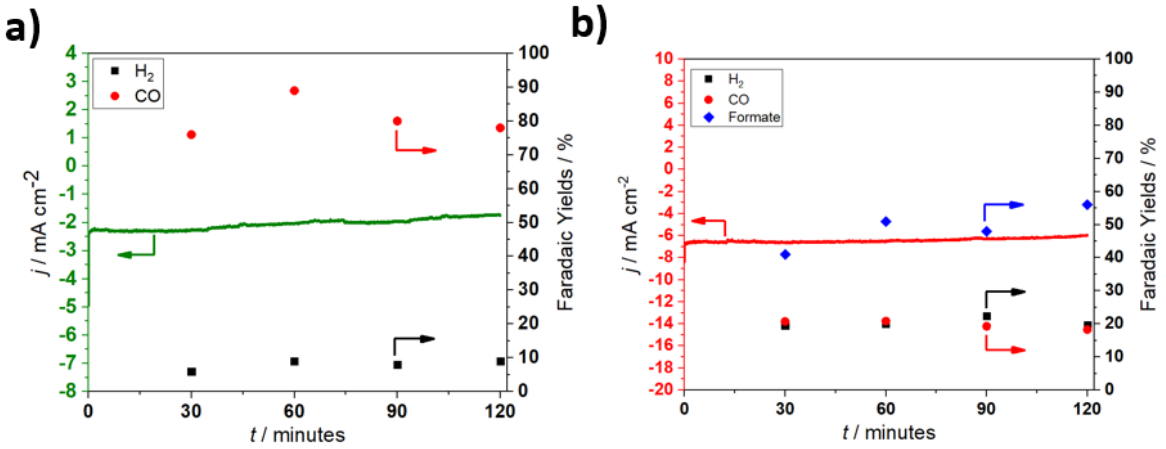

Figure 3: Long-term electrolysis: current density and FY as a function of time during CPE at -1.75 V *vs* Fc/Fc^+ (**a**) and at -1.95 V *vs* Fc/Fc^+ (**b**) under CO_2 in 5% v/v H_2O/EMIM using the HPC@Re/GDL. Faradaic yields for CO (red dots), H_2 (black squares) and formate (blue diamonds).

Conclusion

We have developed a novel hybrid solid catalyst, HPC@Re, for CO_2 electroreduction to CO and HCOOH. Thanks to the hierarchical porosity of the porous and conductive carbon material HPC, large amounts of the molecular catalyst [Re(bpy)$(CO)_3$Cl] can be easily immobilized without any functionalization. We anticipate that HPC can be further used for heterogeneization of other complexes. In order to optimize catalysis, CO_2 electroreduction has been studied in an ionic liquid electrolyte in the presence of water, known to favour CO_2 solubility and activation. To the best of our knowledge, this is the first example of a heterogenized molecular complex characterized for CO_2 reduction catalysis in an ionic liquid. HPC@Re/GDL electrodes thus provide high current densities (up to 11 $mA.cm^{-2}$), high $TOF_{CO+HCOOH}$ (2.3 s^{-1}) and display good stability. When compared to other hybrid solid electrodes in which [Re(bpy)$(CO)_3$Cl] has been immobilized,[6–15] the HPC@Re/GDL electrode is among the most efficient and stable ones. In addition, this novel electrode is unique in providing not only CO but also HCOOH as CO_2 reduction products, with FY(H_2) not exceeding 20%, in marked contrast with the other comparable systems which are selective for CO production and in contrast with the homogeneous catalyst which favours proton reduction over CO_2 reduction and is quite inefficient in the same water/ionic liquid system. The CO/HCOOH ratio can be tuned with the applied potential since it decreased as the potential is shifted to more cathodic values. The combination of a water/ionic liquid electrolyte system, the hierarchical porosity of the support facilitating mass exchange and transfer,[25] and the hydrophobic environment provided by the pores in which the molecular complex is fixed is likely to explain the remarkable and unique performances of HPC@Re as a CO_2 reduction catalyst. However, further studies are required to understand how the support drives and controls the reactivity of the immobilized complex.

Experimental section

General methods

All chemicals were received from commercial sources and used as received. Zinc nitrate hexahydrate ($Zn(NO_3)\cdot 6H_2O$, 99%), 2-methyilimidazole (98%), tetrabutylammonium hexafluorophosphate ($TBAPF_6$, 98%), Nafion© perfluorinated resin (10 µL of a 5 wt% solution in mixture of lower aliphatic alcohols containing 5% water), absolute ethanol (CH_3CH_2OH), methanol (CH_3OH, 99%), dichloromethane (CH_2Cl_2, 99 %), acetonitrile (CH_3CN, 99.8%), chloroform-d ($CDCl_3$, 99.8%) and ammonia solution ($NH_3\cdot H_2O$, 32%) were purchased from Sigma-Aldrich. 1-Ethyl-3-methylimidazolium tetrafluoroborate (>98%) was purchased from IOLITEC Ionic liquid technologies GmbH. $[Re(bpy)(CO)_3Cl]$ was synthesized as previously reported by Kubiak *et al.*[26]

UV−vis spectra were recorded using a Cary 100 UV−vis spectrophotometer (Agilent). ^1H spectra were recorded on a Bruker Avance-III 300 NMR spectrometer (300 MHz) at room temperature. The Rhenium concentrations in the electrolyte were assessed using an Agilent 7900 quadrupole ICP-MS. Liquid samples were sprayed through a micro-nebulizer in a Scott spray chamber prior to ionization. An indium internal standard was injected after inline mixing with the samples to correct for signal drift. Calibration solutions with Re concentrations encompassing the full range of sample concentrations were used to convert measured counts to concentrations. Reported uncertainties were calculated using algebraic propagation of blank substraction and sample count standard deviations (n=3).

Material characterization

Scanning electron microscope (SEM) images were performed by using a JEOL 7500F microscope operating at 15kV with EDX detector incorporated and a Hitachi S-4800 operating at 5kV. X-ray diffraction (XRD) characterization was carried out by Panalytical X'Pert PRO diffractometer (Cu Kα radiation, Bragg-Brentano geometry, sealed tube operated at 45 mA 30 kV X'Celerator linear detector). Nitrogen physisorption analyses were performed with ASAP 2420 using a platinum resistance device and liquid nitrogen as adsorbed molecule.

Synthesis of HPZIF8

Polystyrene spheres (PS) (the size of 400 nm) were synthesized as previously reported[16] and used as a template for the preparation of a hierarchical porous ZIF8 (HPZIF8). HPZIF8 with polystyrene (HPZIF8@PS) was also prepared using a protocol from Chen *et al.*[16], via infiltration of the ZIF8 precursor into the PS spheres template. The following steps were modified from the previous protocol to obtain the HPZIF8. This, was prepared from

HPZIF8@PS treating it at 450 °C during 4 hours under Argon atmosphere for removing the PS beads.

Synthesis of HPC

The hierarchical porous carbon (HPC) derived from ZIF8 was obtained by heating the HPZIF8 at 800 °C during 3 hours under Argon atmosphere. The HPC was used without further treatment.

Preparation of HPC@Re

The preparation of Re complex loading on HPC material was carried out as follows: the solution of [Re(bpy)$(CO)_3$Cl] (6 mg) in CH_2Cl_2 (10 mL) was added dropwise to a sonicated dispersion of HPC (50 mg) in CH_2Cl_2 (20 mL). The suspension was then centrifuged for removing the supernatant. The obtained material was then dried overnight under vacuum condition at room temperature and used without further treatments.

These materials were characterized by: N_2 physisorption analyses, SEM images, EDX mapping and XRD (Supporting Information).

The amount of Re complex loaded was quantified by UV-Visible spectroscopy (Figure S6): after extraction of 30 mg of HPC@Re with 20 mL of CH_2Cl_2 the solution was analysed for its absorption at 387 nm, characteristic of [Re(bpy)$(CO)_3$Cl] and the latter was compared to calibration curve prepared with pure [Re(bpy)$(CO)_3$Cl]. HPC@Re was also treated with $CDCl_3$ for extraction of the complex and characterization by ^{1}H NMR (Figure S5), in order to confirm the integrity of the complex.

Electrode preparation

HPC@Re (5 mg) was sonicated 1 hour in absolute ethanol (200 µL) and a solution of Nafion perfluorinated resin (10 µL of a 5 wt% solution in mixture of lower aliphatic alcohols containing 5% water). The suspension was then, carefully, deposited by drop casting on a gas-diffusion Layer, GDL (AVCarb GDS 3250; 1 cm^2) in order to have a uniform deposition. The electrode was then dried in air overnight at room temperature. For all the experiments the working electrodes were prepared in the same way.

Electrode characterization

SEM images of the HPC@Re/GDL electrode were obtained before and after 2 hours electrolysis. The amount of Re complex present on the GDL was quantified by UV-Visible spectroscopy as described above via extraction of the complex from the HPC@Re/GDL electrode immersed in 20 mL of CH_2Cl_2 (Figure S6) and quantification by comparison with the calibration curve.

Electrochemical characterization

All electrochemical characterization and electrolysis experiments were carried out using a Bio-logic SP300 potentiostat with two-compartment cell with an Ag/AgCl/3M KCl reference electrode, placed in the same compartment as the working HPC@Re/GDL electrode. A platinum counter electrode was placed in a separate compartment. The two compartments were separated by a membrane (Fumasep FBM-Bipolar Membrane). The electrolyte was CO_2-saturated 5% v/v H_2O/EMIM (12.5 mL). The electrochemical cell was first purged with CO_2 at a flow rate of 20 $mL.min^{-1}$ for 1 h prior to catalytic tests using a mass flow controller (Bronkhorst EL-FLOW model F-201CV). All potential values are given versus the potential of the Fc/Fc^+ couple added as an internal standard to the solution after measurement. In 5% v/v H_2O/EMIM: $E1/2(Fc/Fc^+)$ = 0.35V vs Ag/AgCl (Figure S11)

CVs for the determination of surface density of electrochemically active sites were recorded in CH_3CN, 0.1 M $TBAPF_6$ with a scan rate of 10 $mV.s^{-1}$.

The surface loading (Γ[Re] as $mol.cm^{-2}$) of the catalyst was calculated through the integration of the reoxidation wave in the CV scan (Figure S7) using the equation:

$$\Gamma[Re] = \frac{q}{nFA}$$

where q is the charge (C) obtained from integration of the oxidation wave, *n* the number of electrons in the redox process per Re center (*n* = 1), F is the Faraday constant (96485 $C.mol^{-1}$), and A is the geometrical electrode area (1 cm^2).[27]

The homogeneous electrochemical experiments were carried out under the same conditions described above using the same electrochemical cell. A glassy carbon electrode (1 cm^2) was used as working electrode in a solution 1 mM of $[Re(bpy)(CO)_3Cl]$ in 5% v/v H_2O/EMIM.

H_2 and CO were identified and quantified using a gas chromatograph (SRI 8610C) equipped with a packed Molecular Sieve 5 Å column for permanent gases separation and a packed Haysep-D column for light hydrocarbons separation. Argon (Linde 5.0) was used as carrier gas. A flame ionization detector (FID) coupled to a methanizer was used to quantify CO while a thermal conductivity detector (TCD) was used to quantify H_2. The liquid-phase products were quantified using an ionic exchange chromatography system (883 Basic IC plus; Metrohm).

Acknowledgements

The PhDs of D.G and S.P are financially supported from the European School on Artificial Leaf: Electrodes & Devices (eSCALED) project. This work is part of the eSCALED project which has received funding from the European's Union's Horizon 2020 research and innovation programme under the Marie Sklodowska-Curie grant agreement No 765376.

This research used resources of the Electron Microscopy Service located at the University of Namur. This Service is member of the "Plateforme Technologique Morphologie –Imagerie".

SEM images were also collected by F. Pillier at the Laboratoire Interfaces et Systèmes Electrochimiques.

Parts of this work were supported by IPGP multidisciplinary program PARI, and by Paris–IdF region SESAME Grant no. 12015908.

References

[1] R. Francke, B. Schille, M. Roemelt, *Chem. Rev.* **2018**, *118*, 4631–4701.

[2] H. Takeda, C. Cometto, O. Ishitani, M. Robert, *ACS Catal.* **2017**, *7*, 70–88.

[3] N. Elgrishi, M. B. Chambers, X. Wang, M. Fontecave, *Chem. Soc. Rev.* **2017**, *46*, 761–796.

[4] C. Sun, R. Gobetto, C. Nervi, *New J. Chem.* **2016**, *40*, 5656–5661.

[5] L. Sun, V. Reddu, A. C. Fisher, X. Wang, *Energy Environ. Sci.* **2020**, *13*, 374–403.

[6] T. R. O'Toole, L. D. Margerum, T. D. Westmoreland, W. J. Vining, R. W. Murray, T. J. Meyer, *J. Chem. Soc.{,} Chem. Commun.* **1985**, 1416–1417.

[7] C. R. Cabrera, H. D. Abruña, *J. Electroanal. Chem. Interfacial Electrochem.* **1986**, *209*, 101–107.

[8] J. Hawecker, J.-M. Lehn, R. Ziessel, *J. Chem. Soc.{,} Chem. Commun.* **1983**, 536–538.

[9] A. Zhanaidarova, A. L. Ostericher, C. J. Miller, S. C. Jones, C. P. Kubiak, *Organometallics* **2019**, *38*, 1204–1207.

[10] S. Cosnier, A. Deronzier, J.-C. Moutet, *J. Electroanal. Chem. Interfacial Electrochem.* **1986**, *207*, 315–321.

[11] T. Yoshida, K. Tsutsumida, S. Teratani, K. Yasufuku, M. Kaneko, *J. Chem. Soc.{,} Chem. Commun.* **1993**, 631–633.

[12] S. Oh, J. R. Gallagher, J. T. Miller, Y. Surendranath, *J. Am. Chem. Soc.* **2016**, *138*, 1820–1823.

[13] J. Willkomm, E. Bertin, M. Atwa, J.-B. Lin, V. Birss, W. E. Piers, *ACS Appl. Energy Mater.* **2019**, *2*, 2414–2418.

[14] J. D. Blakemore, A. Gupta, J. J. Warren, B. S. Brunschwig, H. B. Gray, *J. Am. Chem. Soc.* **2013**, *135*, 18288–18291.

[15] A. Zhanaidarova, S. C. Jones, E. Despagnet-Ayoub, B. R. Pimentel, C. P. Kubiak, *J. Am. Chem. Soc.* **2019**, *141*, 17270–17277.

[16] K. Shen, L. Zhang, X. Chen, L. Liu, D. Zhang, Y. Han, J. Chen, J. Long, R. Luque, Y. Li, B. Chen, *Science* **2018**, *359*, 206–210.

[17] M. Wu, Y. Li, Z. Deng, B. L. Su, *ChemSusChem* **2011**, *4*, 1481–1488.

[18] S. Suter, S. Haussener, *Energy Environ. Sci.* **2019**, *12*, 1668–1678.

[19] J.-P. Song, L. Wu, W.-D. Dong, C.-F. Li, L.-H. Chen, X. Dai, C. Li, H. Chen, W. Zou, W.-B. Yu, Z.-Y. Hu, J. Liu, H.-E. Wang, Y. Li, B.-L. Su, *Nanoscale* **2019**, *11*, 6970–6981.

[20] M. L. Clark, P. L. Cheung, M. Lessio, E. A. Carter, C. P. Kubiak, *ACS Catal.* **2018**, *8*, 2021–2029.

[21] B. A. Rosen, A. Salehi-Khojin, M. R. Thorson, W. Zhu, D. T. Whipple, P. J. A. Kenis, R. I. Masel, *Science* **2011**, *334*, 643–644.

[22] D. C. Grills, Y. Matsubara, Y. Kuwahara, S. R. Golisz, D. A. Kurtz, B. A. Mello, *J. Phys. Chem. Lett.* **2014**, *5*, 2033–2038.

[23] J. Agarwal, R. P. Johnson, G. Li, *J. Phys. Chem. A* **2011**, *115*, 2877–2881.

[24] A. J. Morris, G. J. Meyer, E. Fujita, *Acc. Chem. Res.* **2009**, *42*, 1983–1994.

[25] X. Zheng, G. Shen, C. Wang, Y. Li, D. Dunphy, T. Hasan, C. J. Brinker, B. L. Su, *Nat.*

Commun. **2017**, *8*, 1–9.
[26] J. M. Smieja, C. P. Kubiak, *Inorg. Chem.* **2010**, *49*, 9283–9289.
[27] B. Reuillard, K. H. Ly, T. E. Rosser, M. F. Kuehnel, I. Zebger, E. Reisner, *J. Am. Chem. Soc.* **2017**, *139*, 14425–14435.